Biosensors and Bioelectronics 87 (2017) 31–37

Contents lists available at ScienceDirect

Biosensors and Bioelectronics

journal homepage: www.elsevier.com/locate/bios

Motor-based microprobe powered by bio-assembled catalase for motion detection of DNA

Yuzhe Xie, Shizhe Fu, Jie Wu*, Jianping Lei, Huangxian Ju

State Key Laboratory of Analytical Chemistry for Life Science, School of Chemistry and Chemical Engineering, Nanjing University, Nanjing 210023, PR China

ARTICLE INFO

Article history:
Received 16 May 2016
Received in revised form
26 July 2016
Accepted 28 July 2016
Available online 30 July 2016

Keywords:
Microprobe
Motor
Catalase
DNA detection
Motion

ABSTRACT

A motor-based microprobe is proposed using a tubular microengine powered by bio-assembled enzyme as catalyst and exploited for washing-free detection of DNA through motion readout. The microprobe is fabricated by assembling a catalase layer on the inner surface of poly(3,4-ethylenedioxythiophene)/Au (PEDOT/Au) microtube through DNA conjugate, which is responsible for the biocatalytic bubble propulsion. The sensing concept of the microprobe relies on the target-induced release of catalase through the DNA strand-replacement hybridization, which decreases the amount of enzyme assembled on microtube to slow down the movement of the microprobe. Therefore, the motion speed is negatively correlated with the target concentration. At the optimal conditions, the microprobe can conveniently distinguish the concentration of specific DNA in a range of 0.5–10 μM without any washing and separation step. This microprobe can be prepared in batch with good reproducibility and stability, and its motion speed can be conveniently visualized by optical microscope. The proposed motor-based microprobe and its dynamic sensing method provide a novel platform for the development of intelligent microprobe and clinical diagnostic strategy.

1. Introduction

As the carrier of genetic information, DNA is the most important genetic material of living beings. The detection of specific DNA fragments can provide useful information for the diagnosis of many genetic disease and cancers (Drummond et al., 2003; Hay Burgess et al., 2006; Risch and Merikangas, 1996; Wang et al., 1997). Various DNA biosensors along with different signal readouts such as electrochemiluminescence, fluorescence, chemiluminescence, colorimetry and electrochemistry have been reported (Feng et al., 2015; Gao and Li, 2013; Li et al., 2016; Ling et al., 2015; Lou et al., 2015; Shen et al., 2012). Although those biosensors have demonstrated good performance, most of them require sophisticated detection instruments and the complexity manufacturing processes, which greatly limit their applications. Therefore, it is a promising way to design new efficient signal transduction platform for DNA detection by utilizing the unique physical properties, for example, analyzing the motion of micromotors.

Micromotors are self-propelled in liquids by converting different sources of energy into mechanical force and motion (Kagan et al., 2012; Mei et al., 2011; Paxton et al., 2004; Peyer et al., 2013; Sanchez et al., 2015; Solovev et al., 2009), and display a high speed and power, good stability, precise motion control, and self-mixing ability (Gao et al., 2012a, 2012b; Guix et al., 2014; Patra et al., 2013; Wang and Pumera, 2015) in recognizing, transporting, and isolating of a wide range of target biomaterials (Campuzano et al., 2012; Orozco et al., 2013a, 2013b). Recently, powerful synthetic self-propelled nano/micromotors offer considerable promise for developing bioanalytical and biosensing protocols (Bunea et al., 2015; Campuzano et al., 2011; Guix et al., 2014; Wang, 2016; Wang and Pumera, 2015) because the motion sensing platform does not require sophisticated analytical instruments and potentially offers spatial resolution. The idea of motion as a transduction mechanism was firstly introduced by Wang and co-workers (Kagan et al., 2009) and adopted to design the motion-based biosensor for detection of DNA and RNA with a bimetallic nanorod (Wu et al., 2010). To address the limitation of catalytic nanowire motors in high ionic-strength media (Paxton et al., 2006; Sanchez et al., 2015), bubble-propelled tubular micromotors have been designed for the detection of natural toxin and heavy metal ions through their inhibition to catalase (Orozco et al., 2013a, 2013b), cancer biomarkers (Yu et al., 2014) and nucleic acids (Nguyen and Minteer, 2015) due to their efficient bubble-induced propulsion in relevant biological fluids (Gao et al., 2011; Mei et al., 2008). However, the biorecognition layer constructed on the micromotors by the self-assembly of the alkanethiol monolayer and covalent coupling of bioreceptors leads to a significant inhibition to the catalytic layer (Balasubramanian et al., 2011; Campuzano et al.,

* Corresponding author.
E-mail address: wujie@nju.edu.cn (J. Wu).

http://dx.doi.org/10.1016/j.bios.2016.07.104
0956-5663/

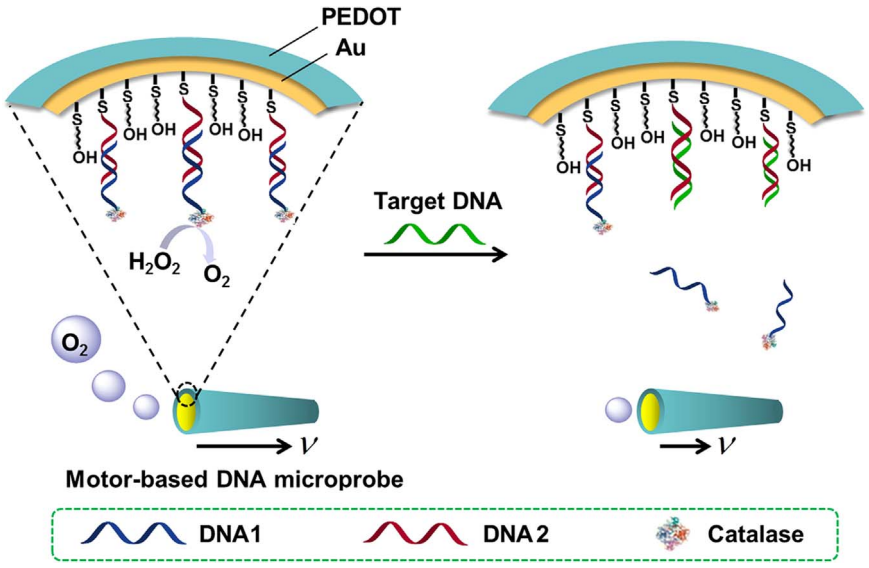

Scheme 1. Schematic representation of motor-based microprobe for DNA detection via motion speed change.

2012). Moreover, the motor-based detection protocol for DNA analysis mostly relies on a sandwich identification assay (Nguyen and Minteer, 2015), which is complex and relatively costly. Here, we use catalase-labeled DNA to present an alternative design of the motor-based DNA microprobe for identification of specific DNA sequence.

Comparing with Pt nanoparticle, catalase as catalyst has higher activity to drive the motion of micromotors through a bubble-induced propulsion mechanism, in which hydrogen peroxide is decomposed to form oxygen gas (Sanchez et al., 2010). In this work, a motor-based microprobe is fabricated by assembly of a catalase layer on the inner surface of poly(3,4-ethylenedioxythiophene)/Au (PEDOT/Au) microtube through DNA conjugate. The motion signal of microprobe is responsible for the biocatalytic bubble propulsion, which can be regulated by the target molecule (Scheme 1). In the presence of target DNA, the DNA1-catalase conjugate is displaced by target DNA, which decreases the amount of enzyme assembled on microtube, and leads to a decrease of the motion speed of microprobe. Thus, a method for convenient and dynamic label-free detection of specific DNA fragments is developed by motion readout. This motor-based microprobe as well as the motion-based detection protocol can be conveniently combined with the developed signal amplification strategies to improve its sensitivity, and extended to detect other analytes such as small molecules and proteins.

2. Materials and methods

2.1. Materials and reagents

3,4-ethylenedioxythiophene (EDOT), 1-ethyl-3-(3-dimethylaminopropyl) carbodiimide hydrochloride (EDC), N-hydroxycinimide (NHS), tris (2-carboxyethyl) phosphine hydrochloride (TCEP), 6-mercapto-1-hexanol (MCH), brilliant blue R and catalase from bovine liver were purchased from Sigma-Aldrich Chemical Co. (St. Louis, MO, USA). Gold plating solution was gifted by Professor Wang Wei at Harbin Institute of Technology (Shenzhen). Sodium cholate hydrate was purchased from Alfa Aesar China Ltd. Sodium dodecyl sulfate (SDS) was obtained from Shanghai Reagent Co. (Shanghai, China). TE buffer (10 mM, pH 7.4) was used to prepare oligonucleotide stock solutions. Phosphate-buffered saline (PBS, 10 mM, pH 5.5) was used as coupling buffer for the immobilization of catalase. Blocking buffer, which was used to block the residual reactive sites on the DNA-modified microtube, was 10 mM PBS (pH 7.4) containing 1 mM MCH. Washing buffer was 10 mM PBS (pH 7.4) spiked with 0.05 wt% SDS. Other reagents were of analytical grade and used as received. Ultrapure water obtained from a Millipore water purification system ($\geq$ 18 MΩ, Milli-Q, Millipore) was used in all experiments. The oligonucleotides with the following sequences were purchased from Shanghai Sangon Biotechnology Co. Ltd. (China) and purified by high-performance liquid chromatography. Their sequences were as follows:

DNA1: 5′-HOOC-TTTTTTTGGTAAAGATGG-3′
DNA2: 5′-HS-TTTTTTCCATCTTTACCAGACAGTGTTA-3′
target DNA: 5′-TAACACTGTCTGGTAAAGATGG-3′
non-complementary DNA: 5′-GATTCGATCTCGACTTCGCATGTACG-3′
single-base mismatch DNA: 5′-TAACAGTGTCTGGTAAAGATGG-3′
three-base mismatch DNA: 5′- TAACAGTGTCTCGTAAACATGG-3′

2.2. Apparatus

Template-assisted electrochemical growth of polymer was carried out with a CHI660B electrochemical workstation (CH Instruments Inc., USA). The morphology of the microprobe was examined with scanning electron microscope (SEM) (Hitachi S-4800, Japan). Zeta potential analysis was performed on Zetasizer (Nano-Z, Malvern, UK). Polyacrylamide gel electrophoresis (PAGE) analysis was performed on an electrophoresis analyser (Bio-Rad, USA) and imaged on Bio-rad ChemDoc XRS (Bio-Rad, USA). The images and videos were captured by Leica DMI 3000B inverted microscope equipped with a Photometrics Evolve 512/SC camera (Roper Scientific, Duluth, GA), and acquired at a frame rate of 10 frames/s using the Leica MM AF 1.5 software.

2.3. Preparation of PEDOT/Au microtubes

The PEDOT/Au microtubes were prepared using a common template-directed electrodeposition protocol (Gao et al., 2012a, 2012b). Briefly, a polycarbonate membrane with 5-μm-diameter micropores (Catalog No 7060-2513, Whatman, U.S.A) was employed as the template. A gold film with a thickness of 75 nm was firstly sputtered on one side of the porous membrane, which was then assembled in a plating cell with an aluminum foil to serve as

a working electrode. On the wall of the micropores, poly(3,4-ethylenedioxythiophene) (PEDOT) was prepared with electropolymerization at +0.80 V to a charge of 0.30 C (vs SCE) in a plating solution containing 15 mM EDOT, 7.5 mM KNO_3 and 100 mM SDS using a Pt wire as counter electrode. Subsequently, the inner Au layer was deposited on the PEDOT galvanostatically at −1.0 mV to a charge of 0.80 C (vs Ag/AgCl) from a gold plating solution, which led to the PEDOT/Au microtubes after the sputtered gold film was removed by polishing with 1 μm alumina slurry, and the template membrane was dissolved in methylene chloride for 15 min. The PEDOT/Au microtubes were collected by centrifugation and washed repeatedly with methylene chloride, ethanol, and ultrapure water. The microtubes were finally collected and stored in ultrapure water at room temperature.

2.4. Fabrication of motor-based microprobe

The fabrication of motor-based microprobe was described as follows. After the mixture of 20 μM DNA1 and 20 μM DNA2 was incubated in hybridization buffer (pH 7.0) containing 50 mM NaCl and 20 mM TCEP for 1 h at room temperature to form DNA duplex, the PEDOT/Au microtubes were incubated in the mixture overnight, which led to the modification of DNA duplex on the inner Au surface through Au-S binding. Excess DNA was removed by centrifuging at 6000 rpm for 10 min. Afterward, the modified microtubes were dispersed in blocking buffer containing 1 mM MCH for 1 h to block the free surface of the inner Au layer. After thrice rinsing with water, the microtubes were transferred into the coupling buffer (PBS, 10 mM, pH 5.5) containing EDC (0.4 M) and NHS (0.2 M) to activate the carboxyl group on DNA1 for 30 min activation at 37 °C. The microtubes were collected and incubated in the catalase (3 mg/mL) solution for 7 h at room temperature, resulting in the modification of catalase on DNA1. Finally, the microtubes were washed repeatedly to remove the excess catalase from the solution. Thus the motor-based microprobes were obtained and suspended in pH 7.0 buffer and stored at 4 °C before use. With the optimized electroplating and modification, more than thousands of micromotors could be gotten in one batch, and each of them could serve as a microprobe.

2.5. Detection of target DNA

After the prepared microprobe was incubated with 30 μL target DNA at different concentrations for 30 min to ensure sufficient strand-displacement hybridization, equal volumes (2.0 μL) of the microprobe dispersion, 5% sodium cholate, and 6% hydrogen peroxide were mixed and casted on a glass slide. The movement of microprobe was visualized with an inverted optical microscope. The velocity of microprobe was calculated by tracking the object"s center-to-center displacement from frame to frame. The motion signal of microprobe was negatively correlated with the concentration of target DNA.

3. Results and discussion

3.1. Characterization of PEDOT/Au microtubes

The SEM images of PEDOT/Au microtube were captured to examine the structural morphology. The top and side views of the microtube showed a length of ~13.5 μm and a defined cone tubular geometry with outer diameter of ~5.0 μm and inner opening of ~3.0 μm (Fig. 1A and B). The outer surface of the polymeric microtube was uniform and compact, while the inner surface of Au layer was rough. An energy dispersive X-ray (EDX) spectroscopy analysis was employed to characterize the composition of PEDOT/Au microtubes. These EDX images clearly showed the presence of Au (Fig. 1C), carbon (Fig. 1D) and sulfur (Fig. 1E) within the microtube with a uniform distribution. The overlap image of the three elements in a PEDOT/Au microtube demonstrated the successful synthesis of PEDOT/Au microtubes (Fig. 1F).

3.2. Characterization of motor-based microprobe

A PEDOT polymeric microtube was fabricated to check the nonspecific adsorption of DNA on the outer surface of PEDOT/Au

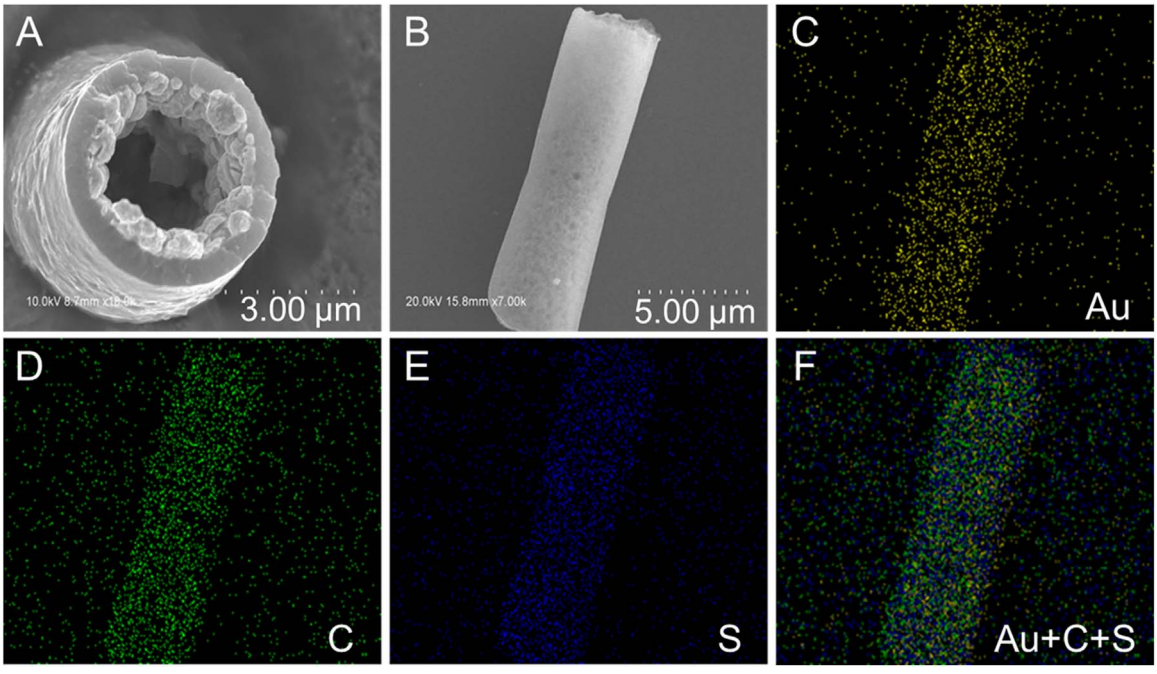

Fig. 1. SEM images of PEDOT/Au microtube from top (A) and side (B) views, and EDX mapping analysis of Au (C), carbon (D), sulfur (E) and the overlap image (F) of three elements in a PEDOT/Au microtube. Scale bars are 3 and 5 μm in (A) and (B–F), respectively.

microtube. The zeta potential analysis indicated that the PEDOT polymeric layer was negatively charged (Fig. S1). Thus, little DNA could be adsorbed on the PEDOT surface due to the electrostatic repulsion. This was verified by the zeta potential of PEDOT microtube after incubation with DNA, which was similar to that of the clean PEDOT tube (Fig. S1). In the process of DNA modification on the surface of Au inner layer of the microtube, the MCH monolayer was introduced to maintain the upstand of DNA strands and minimize the non-specific adsorption of catalase on the surface (Orozco et al., 2013a, 2013b). After incubation in 3 mg/mL catalase solution overnight, the MCH modified microtube did not show any motion movement in the presence of hydrogen peroxide, while the proposed microprobe powered by bio-assembled catalyst layer through DNA conjugate showed a good movement performance (Video S1), indicating catalase did not non-specifically adsorb on the MCH modified inner Au layer.

Supplementary material related to this article can be found online at http://dx.doi.org/1016/j.bios.2016.07.104.

The SEM images were used to characterize the surface of Au inner layer of PEDOT/Au microtubes before and after the modification of DNA-catalase conjugate. Upon the electroplating of Au layer on inner surface of PEDOT, the SEM image showed a rough but clean surface, and some nano granules occurred on the inner layer (Fig. 2A). After the modification of DNA-catalase conjugate, most of the nano granules were covered by a blurry membrane along with slight increased size (Fig. 2B), which looked like the accumulation of protein on the Au surface, indicating the modification of DNA-catalase conjugate onto the Au inner surface and the successful fabrication of the microprobe. PAGE analysis was performed to verify the formation of DNA-catalase conjugate (Fig. 2C and D). Here, the DNA1 was modified with Cy5 (fluorescein) for fluorescent imaging of DNA1 and DNA1-catalase conjugate. The catalase was invisible in gel electrophoresis image (Fig. 2C, lane 1) and the DNA1 exhibited a clearly bright band as control (Fig. 2C, lane 2). The mixture of catalase and DNA1 showed a similar clearly bright band in agreement with the location of the band in lane 2, indicating catalase could not conjugate with DNA1 without EDC-NHS coupling (Fig. 2C, lane 3). On the other hand, catalase and DNA-catalase conjugate were stained by brilliant blue R (Xiang and Lu, 2011). The DNA-catalase conjugate showed a bright fluorescent band at the slow migration position (Fig. 2C, lane 4), which was in agreement with the location of the band in the protein-stained image (Fig. 2D, lane 4′). These results indicated the successful conjugation of DNA1 with catalase through EDC-NHS coupling. In addition, the displacement hybridization of target DNA with DNA1 was also demonstrated through gel electrophoresis analysis (Fig. S2).

3.3. Optimization of preparation and detection conditions

To obtain regular morphology and superior motion performance, the conditions for preparation of motor-based microprobe were firstly optimized. The morphology of the motor-based miroprobe depended on the preparation conditions such as the electropolymerization charge of outer PEDOT layer and inner Au layer. The microtube with little deposition charge of polymer was irregular and deformable because the formed polymer layer was too thin, while the microtube with large deposition charge produced too thick outer polymer to affect the inner opening diameter (Fig. S3). In this work, an optimized deposition charge of 0.3 C was selected for the electropolymerization of PEDOT. In addition, as expected, with the increasing deposition charge, more Au could be electrodeposited on the inner wall of PEDOT (Fig. S4A). When the deposition charge was more than 0.8 C, the thickness of the inner layer affected the inner opening diameter, which led to the lower navigation speed of the microprobe in H_2O_2 solution (Fig. S4B). Thus, 0.8 C was used for the electrodeposition of the inner Au layer.

The DNA concentration used in preparation of the motor-based microprobe was an important factor affecting the motion performance of microprobe. Under the optimal deposition conditions, the optimized concentration was 20 μM (Fig. 3A). As the motion of the microprobe relied on the catalytic generation of oxygen gas produced by catalase, the effect of catalase concentration was examined, which showed the maximum speed at 3 mg/mL (Fig. 3B). The speed of the microprobe also depended on the concentration of H_2O_2 fuel. The average speed increased from 49 ± 16 μm/s at 0.5% H_2O_2 to 411 ± 40 μm/s at 5% H_2O_2, in the presence of 1.6% (w/v) sodium cholate (Fig. 3C and Video S2). To maintain good movement performance of the microprobe and

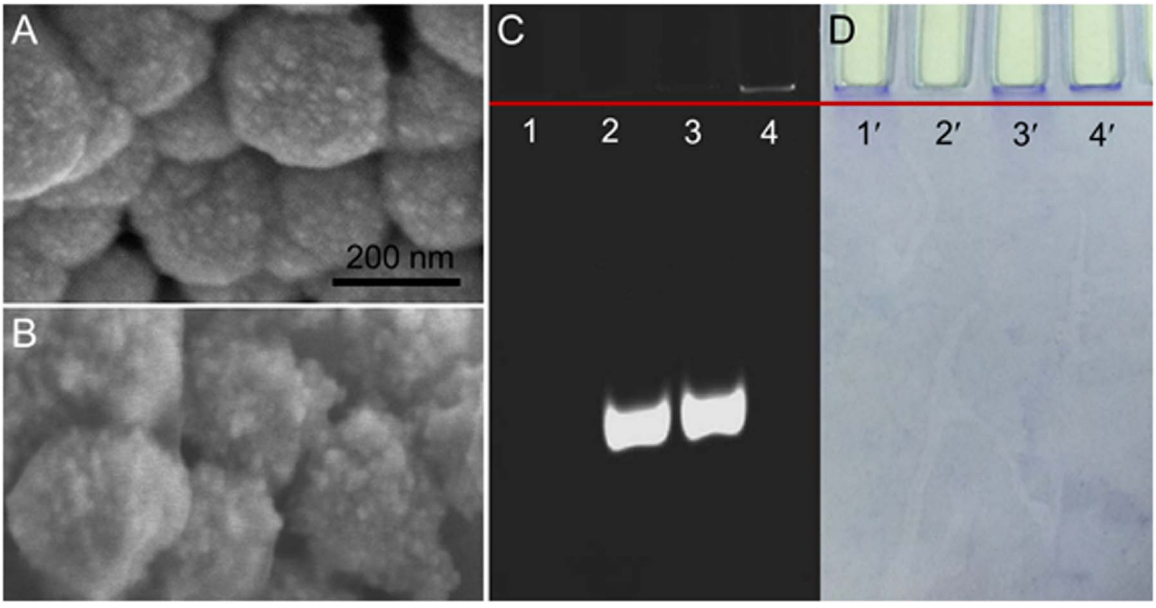

Fig. 2. SEM images of Au inner layer of PEDOT/Au microtube before (A) and after (B) the modification of DNA-catalase conjugate at scale bar of 200 nm. (C) Gel electrophoresis image of catalase (lane 1), DNA1 (lane 2), mixture of catalase and DNA1 (lane 3), and catalase-DNA1 conjugate (lane 4). (D) Protein-staining image of the corresponding lanes in (C) treated with brilliant blue R.

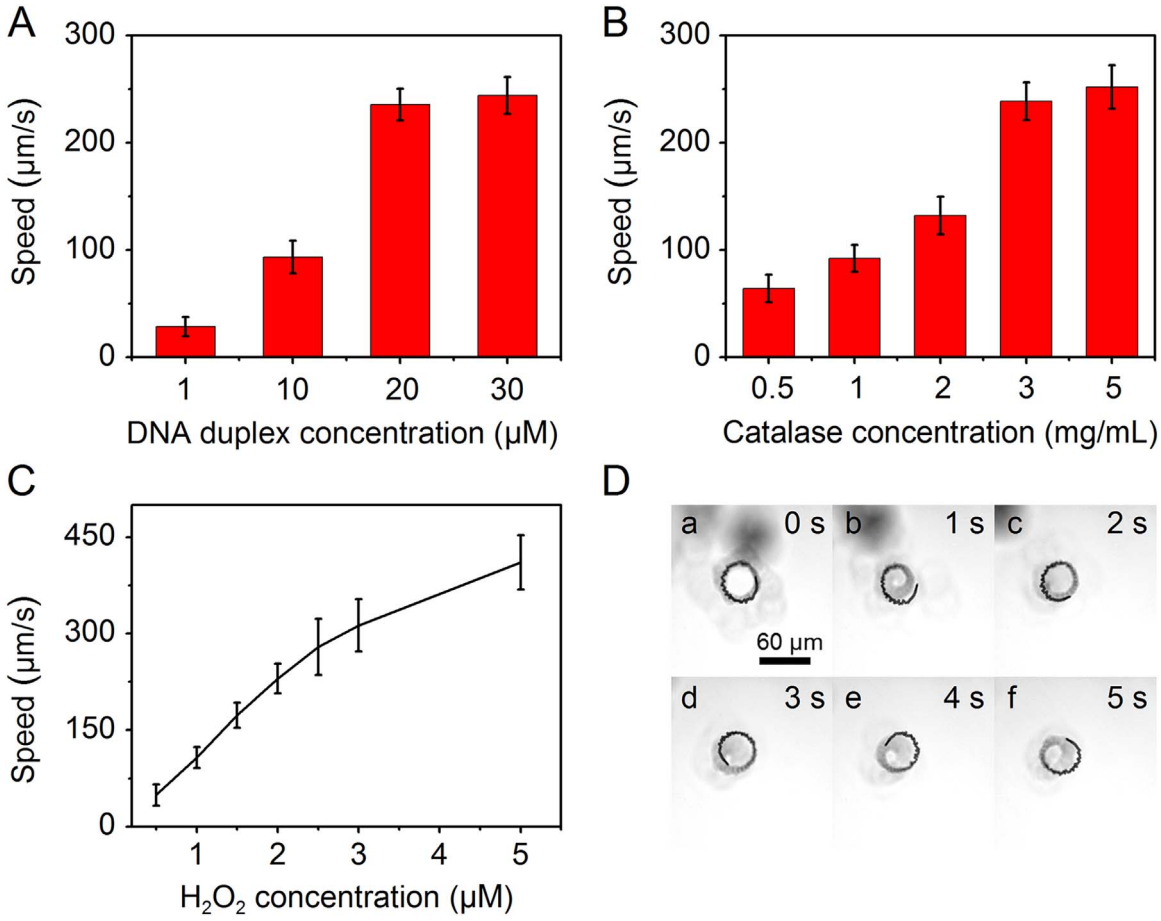

Fig. 3. Motion speed of the microprobe prepared with (A) 1, 10, 20 and 30 μM DNA1 and DNA2, and (B) 0.5, 1.0, 2.0 and 3.0 mg/mL catalase. (C) Dependence of average speed on H_2O_2 concentration. (D) Time-lapse motion images of a microprobe at 0 (a), 1 (b), 2 (c), 3 (d), 4 (e) and 5 s (f) in 2% H_2O_2 solution containing 1.6% (w/v) sodium cholate at scale bar of 60 μm. Error bars represent the standard deviations of speed from 20 microprobes.

good activity of the enzyme modified on microtube, 2% H_2O_2 was used for DNA detection. Time-lapse motion images of a microprobe in 2% H_2O_2 solution containing 1.6% (w/v) sodium cholate demonstrated the high speed and stable motion activity, which was beneficial for bioassay.

Supplementary material related to this article can be found online at http://dx.doi.org/1016/j.bios.2016.07.104.

3.4. Assay performance

The responses of the microprobe motion to different concentrations of target DNA were represented in Fig. 4 and Video S3. With increasing of the DNA concentration, the speed of the microprobe decreased (Fig. 4B). Thus, based on the motion signal, each microprobe could be used as a microsensor to reflect the concentration of target DNA. As shown in Fig. 4B, motion speed response showed low power exponential function relationship with the DNA concentration from 0.5 to 10 μM. The regression

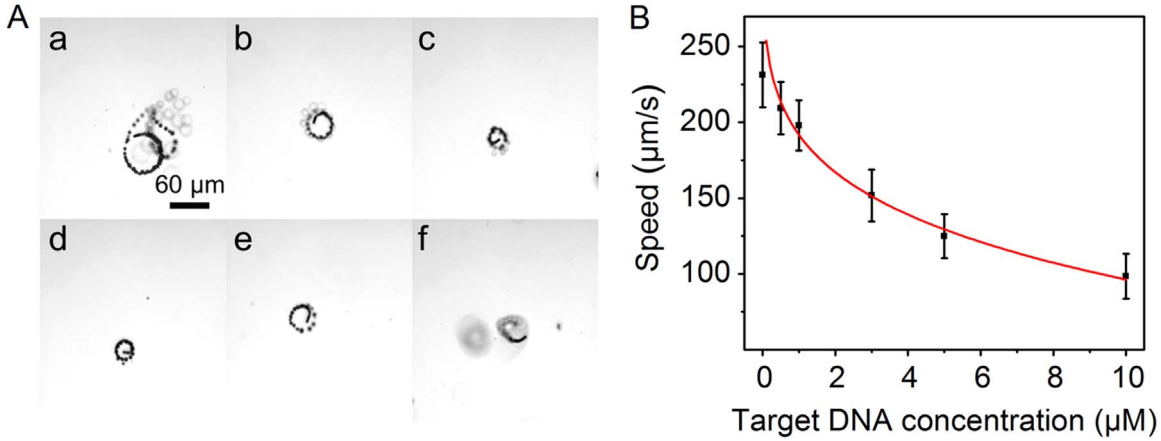

Fig. 4. (A) Time-lapse images of motor-based microprobe in response to 0 (a), 0.5 (b), 1 (c), 3 (d), 5 (e) and 10 μM (f) target DNA in 2% H_2O_2 solution containing 1.6% (w/v) sodium cholate at scale bar of 60 μm. (B) Dependence of average speed on DNA concentration. Error bars represent the standard deviations of speed from 20 microprobes.

equation was $S = 371.9–180.26C^{0.18}$ with the correlation coefficient of 0.982, in which C was the concentration of target DNA. However, it was noted that the exponential value of the motion readout (0.18) was much lower than 1, suggesting the microprobe was suitable for semi-quantitative rather than precise analysis of DNA (Yu et al., 2014). The poor sensitivity of the motion speed upon change of DNA concentration was probably due to the low displacement efficiency between target DNA and DNA duplex in inner layer of the microtube and the limited catalytic performance of the single enzyme label on DNA-conjugate. In order to improve the sensitivity, different signal amplification strategies, for example hybridization chain reaction, could be introduced to construct multi enzyme labels on each DNA-conjugate. In addition, we are trying to develop new open-typed microprobes, in which the biorecognition reaction will occurred in the outer surface of the motor-based microprobe. Furthermore, the sensitivity could be even enhanced by developing a motion-optical based two-way transduction detection model.

Supplementary material related to this article can be found online at http://dx.doi.org/1016/j.bios.2016.07.104.

3.5. Selectivity and stability of microprobe

The specificity of motor-based microprobe for DNA analysis was verified with four different DNA sequences. The target DNA that perfectly matched DNA2 showed a big decrease of motion speed. The proposed microprobe could discriminate the target from three-base mismatched DNA, though it could not discriminate the target from the single-base mismatched DNA. The response of non-complementary DNA was close to that obtained without target DNA (Fig. 5A and Video S4). These results indicated that this microprobe possessed excellent capability to differentiate perfectly matched and mismatched DNA, demonstrating the acceptable selectivity. To test the stability of the microprobe against the storage time, we examined the motion speed of microprobes prepared in one batch every five days. The motion speed had little change even stored at 4 °C after 20 days (Fig. 5B), suggesting that the microprobe could maintain a good catalytic activity and motion performance for a long time at 4 °C. Further speed measurements of the microprobes at different storage times after incubation with 5 μM DNA solution demonstrated that the microprobes could maintain a good stability for DNA detection (Fig. S5). Therefore, the designed motor-based microprobe had a good stability, as those reported in previous work (Orozco et al., 2012). The long-term stability with low apparent discrepancy could be attributed to the immobilization of catalase on the solid support, which minimized the conformational change compared with the free enzyme (Uygun et al., 2015).

Supplementary material related to this article can be found online at http://dx.doi.org/1016/j.bios.2016.07.104.

The reproducibility of microprobe was investigated by using three different batches of the microprobes to detect 3 μM target DNA. All the microprobes were able to sense the target DNA efficiently. The relative standard deviations (RSD) calculated based on twenty microprobes was 14.4%, showing good precision and acceptable fabrication reproducibility of the motor-based microprobe. The relative recovery of this method was evaluated by detecting the DNA concentrations at 4 μM and 8 μM according to the fitted equation obtained above, which were 91.8% and 88.6%, respectively, giving good credibility. To evaluate the practical application of the proposed motor-based probe, the microprobe was used for semi-quantitative analysis of 5 μM DNA spiked in serum sample, which showed a speed of 134 ± 19 μm/s, and the recovery was calculated to be 93.2%. This demonstrated a good performance of the microprobe in complex biological environment and showed promising application.

4. Conclusions

This work successfully proposes a motor-based autonomous microprobe powered by bio-assembled enzyme as catalyst for convenient detection of specific DNA. The DNA microprobe with good motion performance can be conveniently synthesized by template electrodeposition and bio-assembly methods. Regulated by the DNA replace hybridization, the microprobe can be used for semi-quantitation of target DNA without any washing and separation step. The microprobe shows good performance with excellent stability, good selectivity and credibility. Benefitting from the mass production, simple operation and detection, the proposed microprobe shows great potential for point-of-care testing in diverse clinical diagnosis.

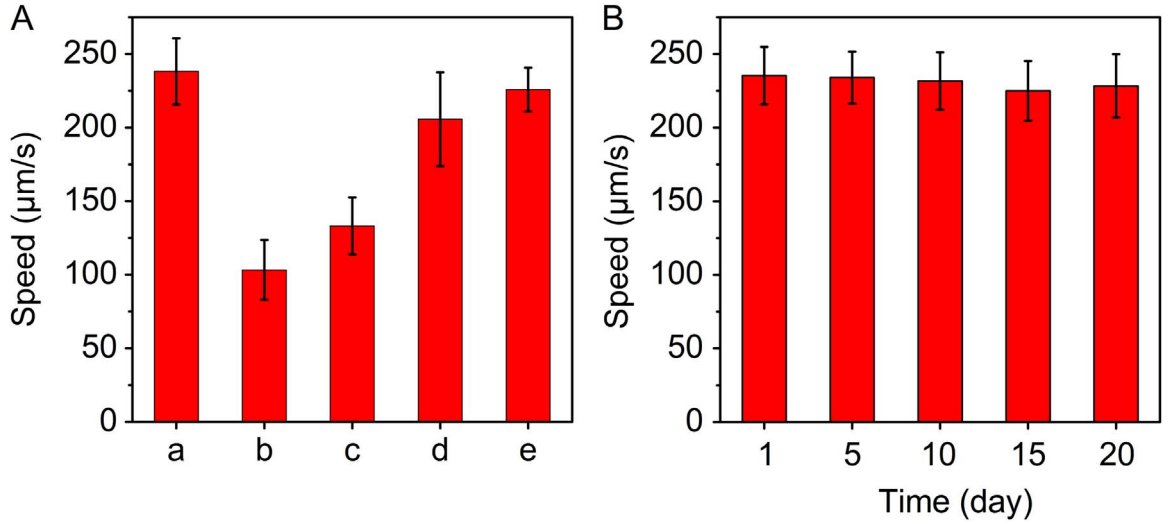

Fig. 5. (A) Average motion speed of microprobe incubated with 2% H_2O_2 solution containing 1.6% (w/v) sodium cholate in (a) absence (b–d) and presence of 5 μM target DNA (b), 50 μM single-base mismatch DNA (c), 50 μM three-base mismatch DNA (d), and 50 μM non-complementary DNA (e), and (B) dependence of average speed on storage time at 4 °C. Error bars represent the standard deviations of speed from 20 microprobes.

Acknowledgement

We gratefully acknowledge the National Natural Science Foundation of China (21575063 and 21361162002), and Independent Research Foundation from State Key Laboratory of Analytical Chemistry for Life Science (5431ZZXM 1504).

Appendix A. Supplementary material

Supplementary data associated with this article can be found in the online version at http://dx.doi.org/10.1016/j.bios.2016.07.104.

References

Balasubramanian, S., Kagan, D., Hu, C.M.J., Campuzano, S., Lobo-Castanon, M.J., Lim, N., Kang, D.Y., Zimmerman, M., Zhang, L.F., Wang, J., 2011. Angew. Chem. Int. Ed. 50, 4161–4164.
Bunea, A.I., Pavel, I.A., David, S., Gáspár, S., 2015. Biosens. Bioelectron. 67, 42–48.
Campuzano, S., Kagan, D., Orozco, J., Wang, J., 2011. Analyst 136, 4621–4630.
Campuzano, S., Orozoc, J., Kagan, D., Guix, M., Gao, W., Sattayasamitsathit, S., Claussen, J.C., Merkoçi, A., Wang, J., 2012. Nano Lett. 12, 396–401.
Drummond, T.G., Hill, M.G., Barton, J.K., 2003. Nat. Biotechnol. 21, 1192–1199.
Feng, Y.Q., Wang, Q.B., Lei, J.P., Ju, H.X., 2015. Biosens. Bioelectron. 73, 7–12.
Gao, Y., Li, B.X., 2013. Anal. Chem. 85, 11494–11500.
Gao, W., Kagan, D., Pak, O.S., Clawson, C., Campuzano, S., Chuluun-Erdene, E., Shipton, E., Fullerton, E.E., Zhang, L.F., Lauga, E., Wang, J., 2012a. Small 8, 460–467.
Gao, W., Sattayasamitsathit, S., Orozco, J., Wang, J., 2011. J. Am. Chem. Soc. 133, 11862–11864.
Gao, W., Sattayasamitsathit, S., Uygun, A., Pei, A., Ponedal, A., Wang, J., 2012b. Nanoscale 4, 2447–2453.
Guix, M., Mayorga-Martinez, C.C., Merkoçi, A., 2014. Chem. Rev. 114, 6285–6322.
Hay Burgess, D.C., Wasserman, J., Dahl, C.A., 2006. Nature 444, 1–2.
Kagan, D., Calvo-Marzal, P., Balasubramanian, S., Sattayasamitsathit, S., Manesh, K. M., Flechsig, G.U., Wang, J., 2009. J. Am. Chem. Soc. 131, 12082–12083.
Kagan, K., Benchimol, M.J., Claussen, J.C., Chuluun-Erdene, E., Esener, S., Wang, J., 2012. Angew. Chem. Int. Ed. 51, 7519–7522.
Li, N., Hao, X., Kang, B.H., Xu, Z., Shi, Y., Lin, N.B., Luo, H.Q., 2016. Biosens. Bioelectron. 77, 525–529.
Ling, P.H., Lei, J.P., Ju, H.X., 2015. Biosens. Bioelectron. 71, 373–379.
Lou, J., Liu, S.S., Tu, W.W., Dai, Z.H., 2015. Anal. Chem. 87, 1145–1151.
Mei, Y.F., Huang, G.S., Solovev, A.A., Bermúdez Ureña, E., Mönch, I., Ding, F., Reindl, T., Fu, R.K.Y., Chu, P.K., Schmidt, O.G., 2008. Adv. Mater. 20, 4085–4090.
Mei, Y.F., Solovev, A.A., Sanchez, S., Schmidt, O.G., 2011. Chem. Soc. Rev. 40, 2109–2119.
Nguyen, K.V., Minteer, S.D., 2015. Chem. Commun. 51, 4782–4784.
Orozco, J., Cortés, A., Cheng, G.Z., Sattayasamitsathit, S., Gao, W., Feng, X.M., Shen, Y. F., Wang, J., 2013a. J. Am. Chem. Soc. 135, 5336–5339.
Orozco, J., García-Gradilla, V., D'Agostino, M., Gao, W., Cortés, A., Wang, J., 2013b. ACS Nano 7, 818–824.
Patra, D., Sengupta, S., Duan, W., Zhang, H., Pavlick, R., Sen, A., 2013. Nanoscale 5, 1273–1283.
Paxton, W.F., Baker, P.T., Kline, T.R., Wang, Y., Mallouk, T.E., Sen, A., 2006. J. Am. Chem. Soc. 128, 14881–14888.
Paxton, W.F., Kistler, K.C., Olmeda, C.C., Sen St., A., Angelo, S.K., Cao, Y.Y., Mallouk, T. E., Lammert, P.E., Crespi, V.H., 2004. J. Am. Chem. Soc. 126, 13424–13431.
Peyer, K.E., Zhang, L., Nelson, B.J., 2013. Nanoscale 5, 1259–1272.
Risch, N., Merikangas, K., 1996. Science 273, 1516–1517.
Sanchez, S., Soler, L., Katuri, J., 2015. Angew. Chem. Int. Ed. 54, 1414–1444.
Sanchez, S., Solovev, A.A., Mei, Y.F., Schmidt, O.G., 2010. J. Am. Chem. Soc. 132, 13144–13145.
Shen, W., Deng, H.M., Gao, Z.Q., 2012. J. Am. Chem. Soc. 134, 14678–14681.
Solovev, A.A., Mei, Y.F., Bermúdez Ureña, E., Huang, G.H., Schmidt, O.G., 2009. Small 5, 1688–1692.
Wang, H., Pumera, M., 2015. Chem. Rev. 115, 8704–8735.
Wang, J., 2016. Biosens. Bioelectron. 76, 234–242.
Wang, J., Rivas, G., Cai, X.H., Dontha, N., Shiraishi, H., Luo, D.B., Valera, F.S., 1997. Anal. Chim. Acta 337, 41–48.
Wu, J., Balasubramanian, S., Kagan, D., Manesh, K.M., Campuzano, S., Wang, J., 2010. Nat. Commun. 1, 1–6.
Xiang, Y., Lu, Y., 2011. Nat. Chem. 3, 697–703.
Yu, X.P., Li, Y.N., Wu, J., Ju, H.X., 2014. Anal. Chem. 86, 4501–4507.